

Wavefront sensing by numerical evaluation of diffracted wavefields

M. Bichra, T.Meinecke, S. Sinzinger

*Fachgebiet Technische Optik, Institut für Mikro- und Nanotechnologien—IMN MacroNano,
Technische Universität Ilmenau,
Ilmenau 98684, Germany
Mohamed.bichra@tu-ilmenau.de*

Abstract:

A novel wavefront sensor principle based on decomposition of the angular spectrum propagator and Fourier analysis is presented. A wavefront is propagated to a 2 dimensional binary cross grating. The appropriate diffraction orders are filtered out and captured by a CCD camera. The following Fourier analysis delivers maps of phase gradients in the x and y coordinates. We verify the presented method by numerical tests and experimentally in a measurement setup on the example of a wavefront generated by a cubic phase element in transmission and reflection. We compared the results of our principle with a commercial Shack-Hartmann wavefront sensor.

Key words: Wavefront sensing, Metrology, Freeform, Testing, Metrological instrumentation

Introduction

The performance of high-precision optical systems with spherical optics is limited by aberrations [1]. The geometrical aberrations can be reduced by using aspheric and free-form optics. At the same time, free-form elements open a wide field of additional functionalities allowing the minimization of the number of required components, size and weight of the system. The fabrication of high-precision free-form surfaces requires new production techniques as well as new appropriate metrology procedures and systems [2][3].

A suitable metrology principle should enable high accuracy, universal application, contactless sensing, low price and short measure time. Ideally the measurement systems should be capable of being integrated into the production line for freeform optical elements. An optical metrology approach provides the potential for surface profiling as well as optical characterization of the element functionality [4].

There exists a wide range of procedures for the precise measurement of wavefronts generated by freeform surfaces. In order to test surface shapes of low complexity, such as flats or spherical surfaces (lenses, mirrors, etc.), interferometry is well established. However, this method has some drawbacks such as the sensitivity to external vibrations and temperature fluctuations, the complexity of the measurement setup and its complicated

alignment. The Shack Hartmann sensing with or without Null test is one of the most widely used principles for the wavefront measurement. But this method offers a relatively poor lateral resolution and the alignment efforts for the Null tests are quite high [4]. Talbot interferometry is one variation of the interferometric measurements with less sensitivity to environmental noise. In contrast to the conventional interferometry this method does not require a separate beam path for the reference wave simplifying the alignment and reducing the requirements to mechanical stability [5][6].

According to a Talbot interferometer proposed by Takeda [6], each of the subspectra of Fourier transformed intensity in the Talbot plane provides the whole wavefront information. When the sub spectra are filtered and shifted to the center, the x,y gradient distributions of the wavefront impinged on the grating can be revealed.

In this paper we demonstrate a modified version of the conventional Talbot interferometer by adding spatial filtering in a corresponding Fourier plane and a following Fourier analysis using simplified representation of the propagator phase.

General Approach

The schematic diagram of the proposed wavefront sensor is shown in Fig. 1. The goal of our experiment is to demonstrate the wavefront analysis using a two-dimensional (2D) binary cross grating. An incoming

arbitrary wavefront resulting, for instance, from the transmission through a specifically shaped test sample hits an amplitude binary cross grating. This grating is placed at the distance z in front of the focal plane of a $4f$ setup which is used to generate an image on a camera sensor. In the Fourier plane of this setup we perform spatial filtering operations in the spectral domain. The camera in the image plane captures an intensity image which is evaluated by the following Fourier analysis.

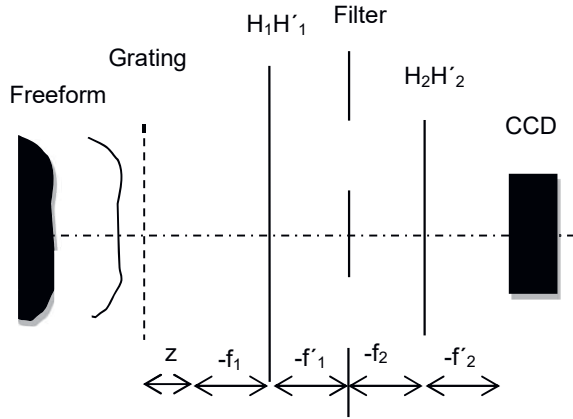


Fig. 1. Schematic diagram of the proposed wavefront sensor.

Simplified Representation of the Propagator Phase

The main idea of our numerical wavefield analysis is the appropriate decomposition of spherical propagator phase in order to simplify the final Fourier analysis. We perform the numerical propagation in the spectral domain using the angular-spectrum method [7]. The modulated signal is multiplied with the propagation kernel of

$$\tilde{P}_z(\omega_x, \omega_y) = \exp(i \varphi_z(\omega_x, \omega_y))$$

The phase φ_z is determined by

$$\varphi_z(\omega_x, \omega_y) = z \sqrt{k^2 - \omega_x^2 - \omega_y^2}$$

with the spatial frequencies of $\omega_{x,y}$ along x,y , respectively and λ as the illumination wavelength.

The two dimensional function $\tilde{P}_z(\omega_x, \omega_y)$ can be imagined as the upper half of a three dimensional ellipsoid on a circular ground of spatial frequencies (ω_x, ω_y) . The actual relationship between the propagator phase and the signal spectrum behind the grating is demonstrated in a cross section in Fig. 2 for the $\pm 1^{\text{st}}$ orders in ω_x and 0^{th} order in ω_y

direction. The -1^{st} , 0^{th} and $+1^{\text{st}}$ orders (replicas) are modulated by different sections of the propagation phase function (different colors).

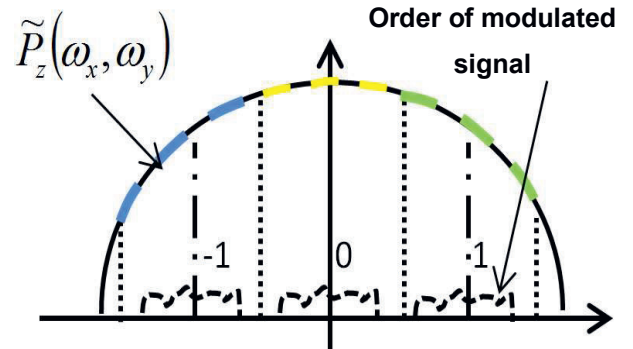


Fig. 2. Illustration of the propagator kernel along the ω_x axis including the -1^{st} , 0^{th} and $+1^{\text{st}}$ order of the signal spectrum behind the grating.

Each replica contains the same information about the signal. Nevertheless, they differ in phase introduced by the propagation. To simplify the following signal evaluation, we represent the propagator from the perspective of spectral replica.

We decompose the actual spherical propagator phase φ_z as follows:

$$\varphi_z(\omega_x, \omega_y)_{q_x \omega_{x0}, q_y \omega_{y0}} \approx \varphi_{z0} + \varphi_{zq} + \varphi_t \cdot \omega(\omega_x, \omega_y)$$

into

- a term of φ_{z0} which corresponds to the spherical propagator phase near the origin, i.e. in the 0^{th} order or without using a cross grating:

$$\begin{aligned} \varphi_{z0}(\omega_x, \omega_y) &= \varphi_z(\omega_x - q_x \omega_{x0}, \omega_y - q_y \omega_{y0}) \\ &= \varphi_z(\Delta \omega_x, \Delta \omega_y) \end{aligned}$$

- an additive offset of φ_{zq} at the replica frequencies of $q_x \omega_{x0}$, $q_y \omega_{y0}$ with $q_{x,y}$ as integer in x,y :

$$\varphi_{zq}(\omega_x, \omega_y) = \varphi_z(q_x \omega_{x0}, q_y \omega_{y0})$$

- and a linear (tangential) term having a slope of

$$\varphi_t(q_x \omega_{x0}, q_y \omega_{y0}) = - \frac{z \lambda \cdot (q_x d_y \cdot q_y d_x)}{\sqrt{(d_x d_y)^2 - (q_x \lambda d_y)^2 - (q_y \lambda d_x)^2}}$$

Derivation of the gradients of signal at the camera plane

The camera captures the intensity. Its spectrum is illustrated in Fig. 3. We choose now the replica of order (2,0) for the further analysis.

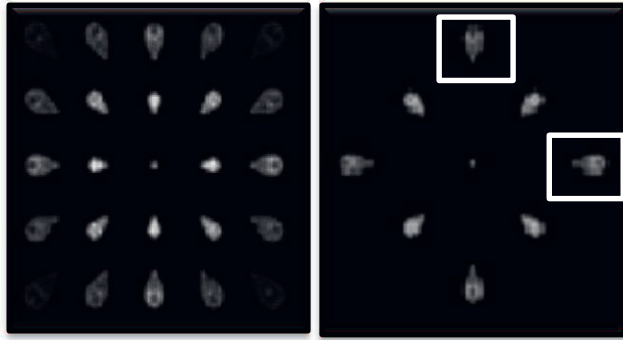


Fig3: Illustration of the spectrum of the intensity captured behind the grating. a: before, b: after spatial filtering in Fourier plane

The partial intensity $I_{2,0}$ which is propagated back from the filtered spectral replica of order (2,0) can be described following Eq.:

$$I_{2,0}(x, y) = \frac{1}{16} A(x - \varphi_t, y) \cdot A(x + \varphi_t, y) \cdot \exp(i[\varphi(x - \varphi_t, y) - \varphi(x + \varphi_t, y)])$$

with $A(x, y)$ as the amplitude. The argument of $I_{2,0}(x, y)$ corresponds to:

$$\Delta\varphi_x(x, y) = \varphi(x - \varphi_t, y) - \varphi(x + \varphi_t, y) = \arg(I_{2,0}(x, y))$$

The gradient $\delta\varphi(x, y)/\delta x$ in x direction can be derived from the differential quotient

$$\frac{\delta\varphi(x, y)}{\delta x} = \lim_{\varphi_t \rightarrow 0} \frac{\varphi(x - \varphi_t, y) - \varphi(x + \varphi_t, y)}{2\varphi_t} \approx -\frac{\sqrt{d_x^2 - \lambda^2}}{2z\lambda} \arg(I_{2,0}(x, y))$$

The derivation of gradient $\delta\varphi(x, y)/\delta y$ in y direction based on the (back transformed) spectral replica of $I_{0,2}(x, y)$ is straight forward.

Experimental Validation

The presented method is tested experimentally on the example of a cubic wavefront generated by a phase plate. Its designed profile is described by a seventh-order polynomial having a maximum sag of 1.119 mm. It has been fabricated on PMMA by ultraprecision machining at the Institute for Micro and Nanotechnologies (IMN) at the Technische Universität Ilmenau in Germany [3]. The used amplitude grating with a grating period of 50 μm for this experiment was fabricated by means of lithography. A LED with a wavelength of $\lambda = 633\text{nm}$ and a pinhole in the focal plane of a lens support the parallel illumination.

We imaged the intensity distribution after the grating onto a CCD U-eye camera with the resolution of 1280x1024 pixels and the pixel size of 5.3 μm. After the determination of the wavefront using the presented algorithm we compared the results with a commercial Shack Hartmann Sensor point by point. Without the spatial filtering in Fourier plane, the deviation to the SHS is 5.23 μm. After applying the Fourier filtering, the deviation is only 0.24 μm due to the suppression of aliasing of adjacent spectral replica orders (fig4).

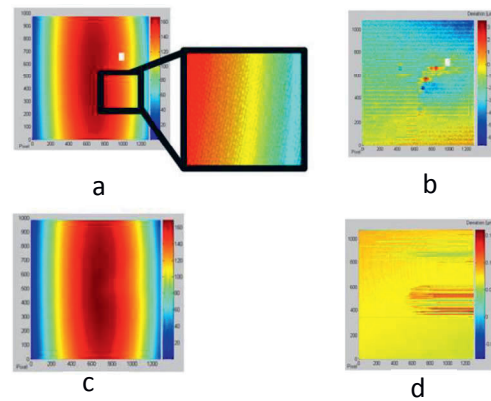


Fig4: a: Reconstructed wavefront without spatial filtering, b: Point by point difference to SHS without spatial filtering c: Reconstructed wavefront including spatial filtering, d: Resulting point by point difference to SHS from c)

Conclusion

In this paper a novel principle of a diffractive wavefront sensor based on the decomposition of the angular spectral propagator is presented. With an appropriate spatial filtering in the Fourier plane, the aliasing effect can be avoided. We tested the system successfully for a wavefront originating from an optical freeform element and validated the results using a SHS.

References

1. X. Zhang, L. Zheng, X. He, L. Wang, and F. Zhang, "Design and fabrication of imaging optical systems with freeform surfaces," Proc. SPIE 8486, 848607 (2012).
2. S. Stoebenau, R. Kleindienst, M. Hofmann, and S. Sinzinger, "Computer aided manufacturing for freeform optical elements by ultra-precision micromachining," Proc. SPIE 8126, 812614 (2011).
3. K. K. Pant, D. R. Burada, M. Bichra, M. P. Singh, A. Ghosh, G. S. Khan, S. Sinzinger, and

- C. Shakher, "Subaperture stitching for measurement of freeform wavefront," *Appl. Opt.* 54, 10022–10028 (2015).
4. G. S. Khan, M. Bichra, A. Grewe, N. Sabitov, K. Mantel, I. Harder, A. Berger, N. Lindlein, and S. Sinzinger, "Metrology of freeform optics using diffractive null elements in Shack–Hartmann sensors," in *3rd EOS Conference on Manufacturing of Optical Components*, Munich, Germany, 2013
 5. M. Bichra, N. Sabitov, and S. Sinzinger, "Wavefront sensor based on modified Talbot effect," in *DGaO Proceedings* (2015)
 6. M. Takeda, I. Hideki, and S. Kobayashi, "Fourier-transform method of fringe-pattern analysis for computer-based topography and interferometry," *J. Opt. Soc. Am.* 72, 156–160 (1982)
 7. Mohamed Bichra, Nail Sabitov, Thomas Meinecke, and Stefan Sinzinger, "Wavefront sensing by numerical evaluation of diffracted wavefields," *Appl. Opt.* 56, A13-A22 (2017)